

Electronic Supplementary Material (ESI) for Green Chemistry. This journal is © The Royal Society of Chemistry

Redox-active and Brønsted Basic Dual Sites for Photocatalytic activation of benzylic C-H bonds based on Pyridinium Derivative

Shuai Ma^a, Jin-Ming Ma^b, Jing-Wang Cui^a, Cai-Hui Rao^a, Meng-Ze Jia^a, Jie Zhang^{a*}

a S. Ma, J. W. Cui, C. H. Rao, M. Z. Jia, Prof. J. Zhang

MOE Key Laboratory of Cluster Science, Beijing Key Laboratory of Photoelectronic/Electrophotonic Conversion Materials

School of Chemistry and Chemical Engineering, Beijing Institute of Technology

Beijing 102488, P. R. China

E-mail: zhangjie68@bit.edu.cn

b J. M. Ma

Hebei Key Laboratory of Applied Chemistry

School of Environmental and Chemical Engineering, Yanshan University

Qinhuangdao 066004, P. R. China

Section 1. Experimental section

1.1 Materials and methods

All of the chemicals were obtained from commercial sources and were used as received unless otherwise stated. IR spectra (KBr pellets) were obtained on a Nicolet IS10 FT-IR spectrometer. The steady-state UV-vis absorption spectra were measured with a Persee TU-1901 Spectrometer. The transient absorption spectra were measured with a Flucent Helios Ultrafast Systems. The electron spin resonance (ESR) signal was collected with JES-FA200 ESR Spectrometer. ^1H NMR spectrum was carried out on a Bruker AV-400 NMR spectrometer. The GC analyses were performed on Shimadzu GC-2014C with an FID detector equipped with an Rtx-5 capillary column. The 365 nm LED light source for light-induced UV-vis absorption spectra and ESR measurements was obtained by MLED4 system from Zolix Instruments Co.,Ltd. Catalysis reactions under 365nm and visible light irradiation ($\lambda > 400$ nm) were carried out by using Beijing Perfectlight Multi-channel photochemical reaction system PCX-50C. The steady-state luminescence quenching spectra were recorded on an Edinburgh FS50 spectrofluorometer (PL) at 365 nm laser excitation at room temperature. Phosphorescence spectra were recorded on an Edinburgh FLS1000 at 365 nm laser excitation at room temperature.

Density functional theory (DFT) calculations were carried out by Gaussian-16 software. The M062X density functional method was employed in this work to perform all the computations. The def2-SVP basis set was used for the atoms in geometry optimizations using the PCM solvation model with acetonitrile as solvent. Vibrational frequency analyses at the same level of theory were performed on all optimized structures to characterize stationary points as local minima or transition states. Furthermore, intrinsic reaction coordinate (IRC) calculations were carried out to confirm that transition state structures connect to the appropriate reactants and products. The single-point energy calculations were carried out using the def2-TZVP basis set to provide better energy correction. [Ref: [1] Gaussian 16, Revision A.03, M. J. Frisch, G. W. Trucks, H. B. Schlegel, et al., Gaussian, Inc., Wallingford CT,

2016; [2] Zhao Y, Truhlar D. G, *Theor Chem. Acc.* 2008, 120, 215–241; [3] Weigend, F.; Ahlrichs, R. *Phys. Chem. Chem. Phys.* **2005**, 7, 3297– 3305]

1.2 The NMR and IR details of electron-relay mediators

TPT: IR (KBr pellet, cm^{-1}): 3039(w), 1577(m), 1511(s), 1373(s), 1317(w), 1052(w), 991(w), 800 (s), 642(s), 509(m). **TTMBPY·3Br:** IR (KBr pellet, cm^{-1}): 3409(s), 3112(w), 3039(m), 2948(w), 1716(s), 1639(m), 1529(s), 1444(s), 1436(w), 1374(s), 1286(s), 1130(m), 1089(m), 1047(w), 1006(w), 954(w), 817(m), 761(m), 711(w), 669(w), 518(w). ^1H NMR (400 MHz, DMSO) δ 9.69 (d, $J = 6.8$ Hz, 2H), 9.58 (d, $J = 6.8$ Hz, 2H), 7.79 (d, $J = 7.7$ Hz, 1H), 7.62-7.70 (m, 3H), 7.53 (t, $J = 7.6$ Hz, 1H), 7.42 (d, $J = 8.2$ Hz, 3H), 6.14 (s, 2H), 3.61 (s, 3H). **TTEPY·3Br:** IR (KBr pellet, cm^{-1}): 3405(s), 3116(w), 3039(m), 1640(m), 1585(w), 1527(s), 1456(w), 1370 (s), 1323(w), 1176(w), 823(m), 748(w), 530(w) ^1H NMR (400 MHz, DMSO) δ 9.56 (s, 4H), 4.86 (d, $J = 7.2$ Hz, 2H), 1.68 (t, $J = 7.3$ Hz, 3H).

Section 2. Additional data and figures

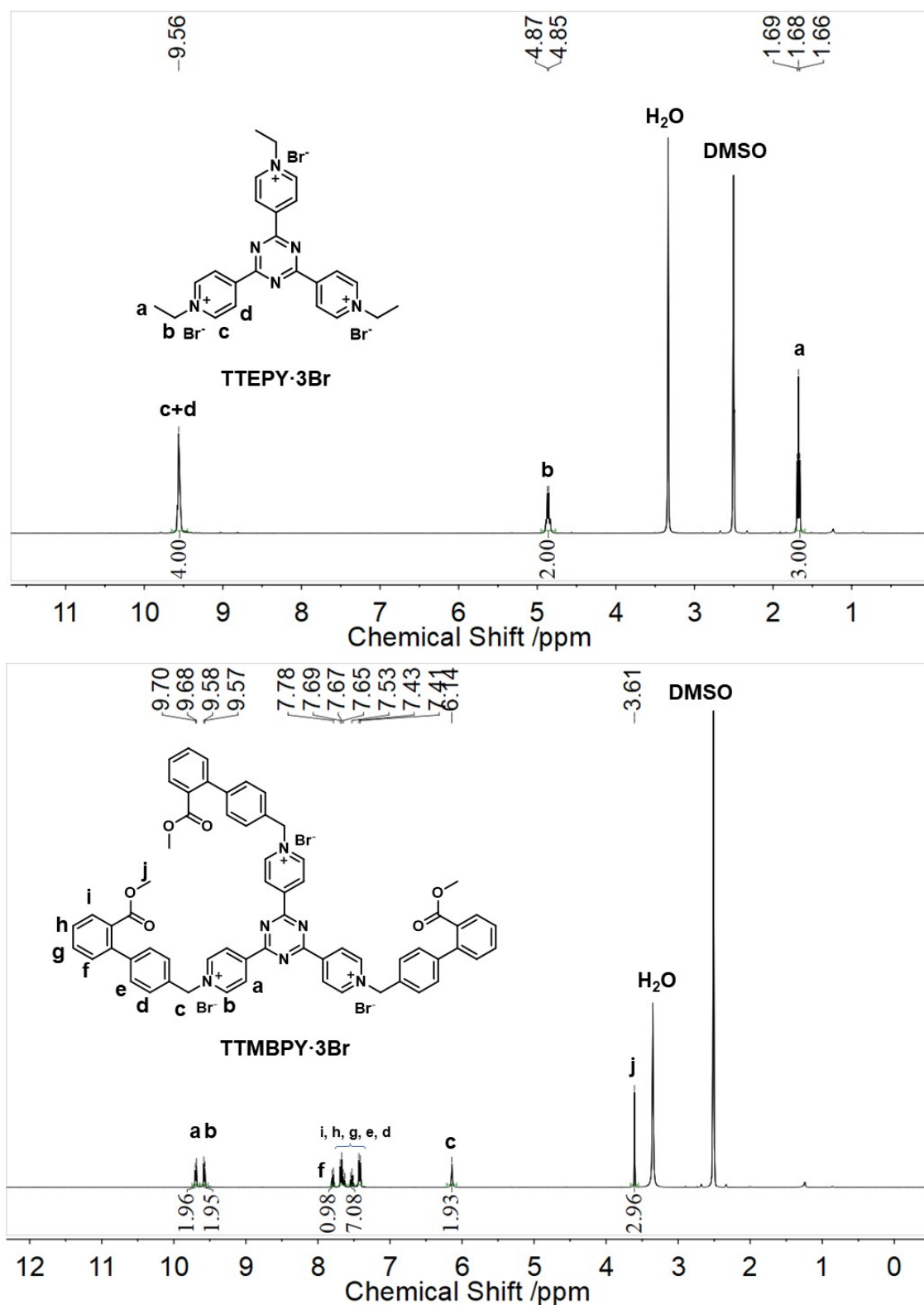


Figure S1. ^1H NMR spectra of TTEPY·3Br and TTMBPY·3Br in DMSO-d_6

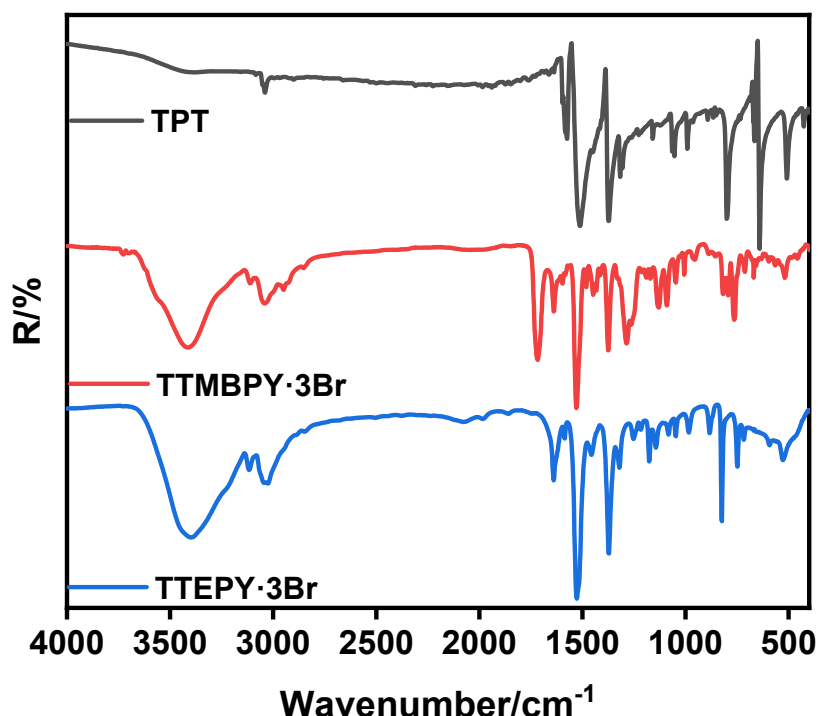


Figure S2. FT-IR spectra of TPT, TTMBPY·3Br and TTEPY·3Br.

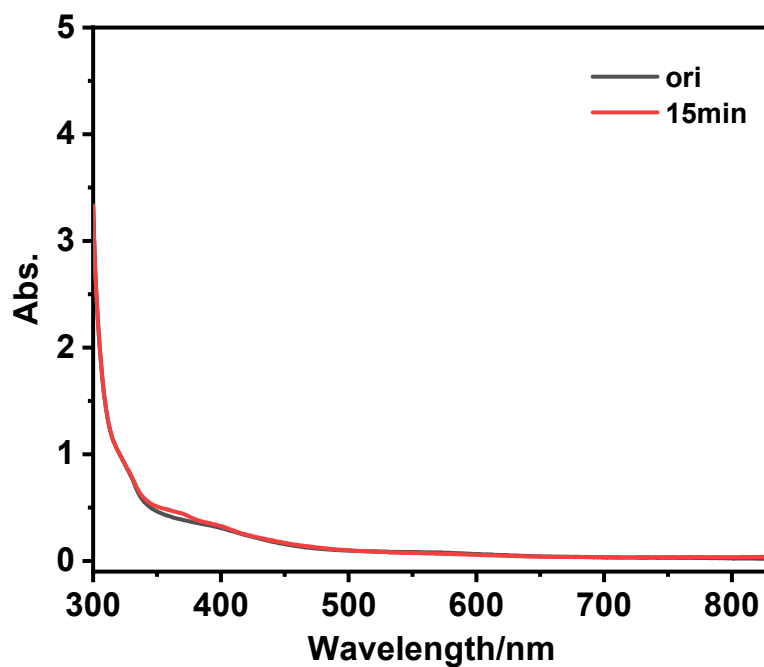


Figure S3. UV-vis spectral evolution of TTEPY·3Br (5×10^{-4} M) in N₂-saturated MeCN solution upon 365 nm light irradiation.

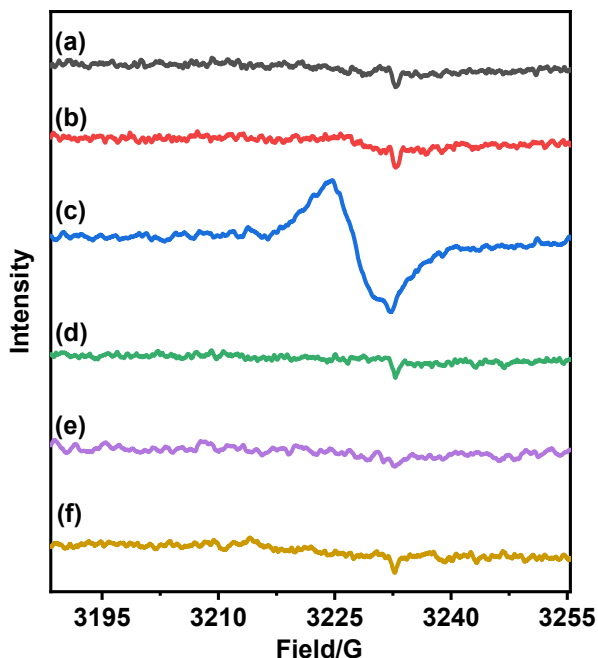


Figure S4. The ESR spectral changes of the mixture of TTEPY·3Br and ethylbenzene in MeCN under 365 nm light irradiation: (a) the original state in air; (b) after irradiation under air atmosphere; (c) after irradiation under N₂ atmosphere; (d) exposure to air after irradiation under N₂ atmosphere; (e) MeCN without TTEPY·3Br under 365 nm light irradiation under N₂ atmosphere; (f) Ethylbenzene in MeCN without TTEPY·3Br under 365 nm light irradiation under N₂ atmosphere.

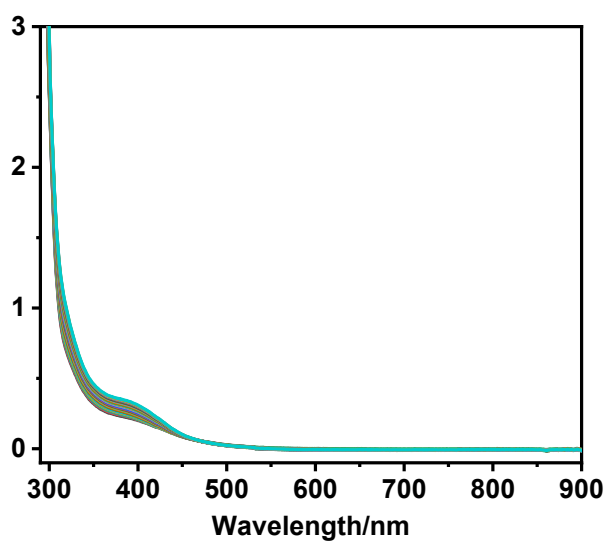


Figure S5. UV-vis spectral change of TTEPY·3Br (5×10^{-4} M) and ethylbenzene (0.5 M) in MeCN under air atmosphere upon 365 nm light irradiation for 15min.

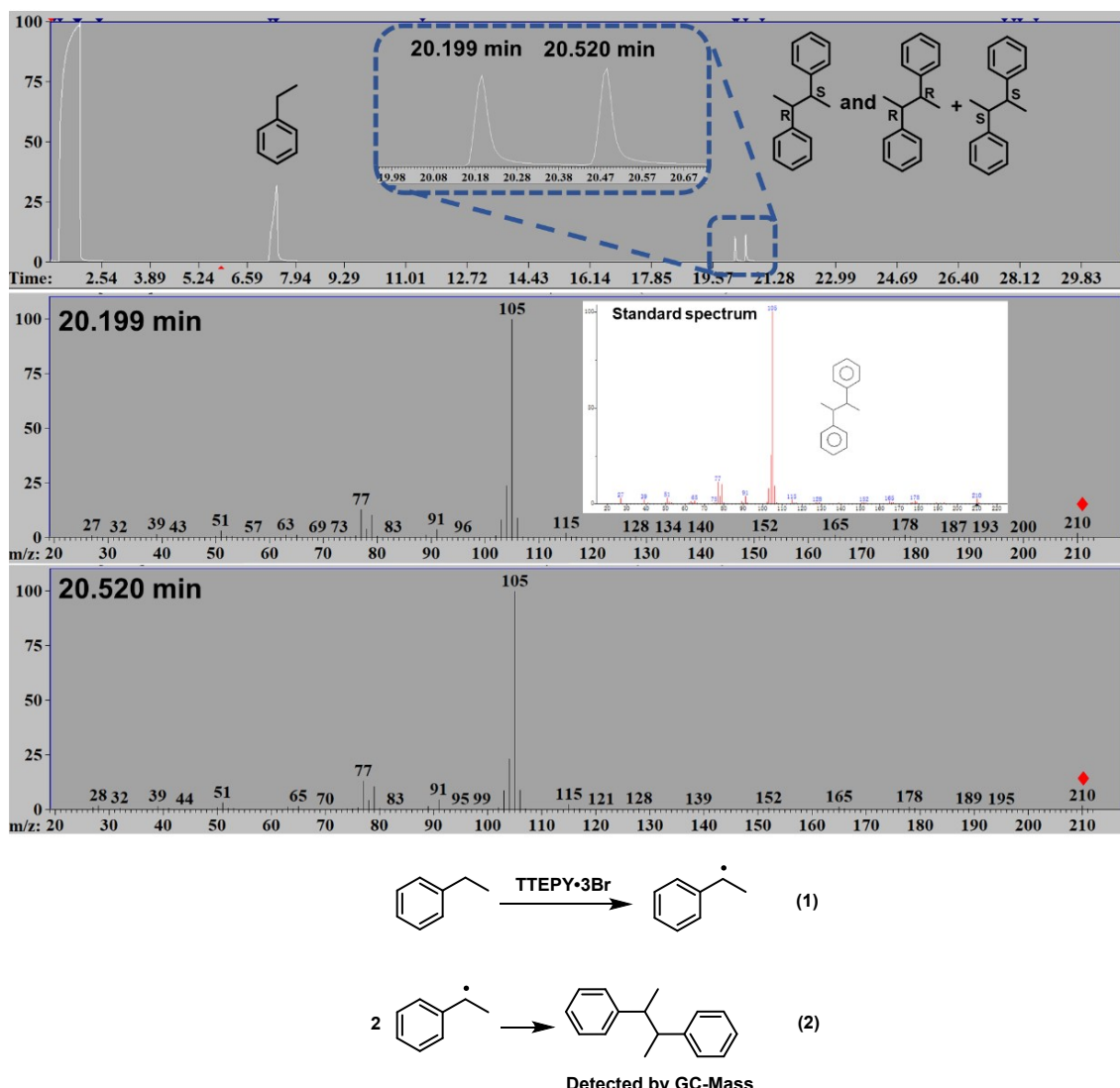


Figure S6. GC-Mass trace of crude reaction mixture of the photochemical reaction of ethylbenzene under N₂ atmosphere.

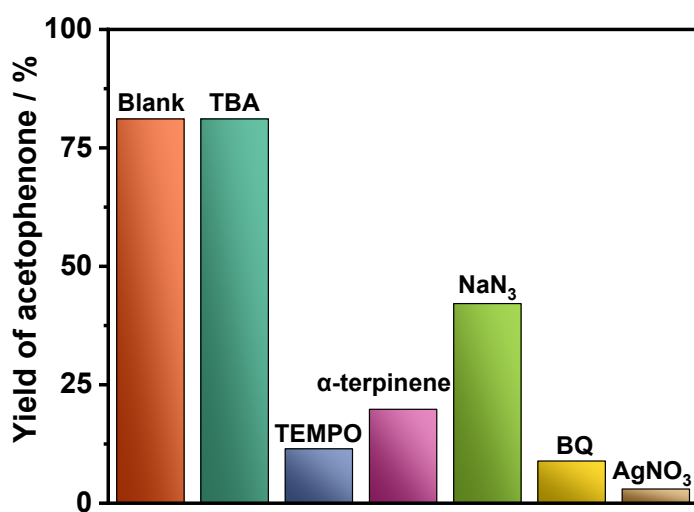


Figure S7. Oxidation of ethylbenzene in the presence of different scavengers.

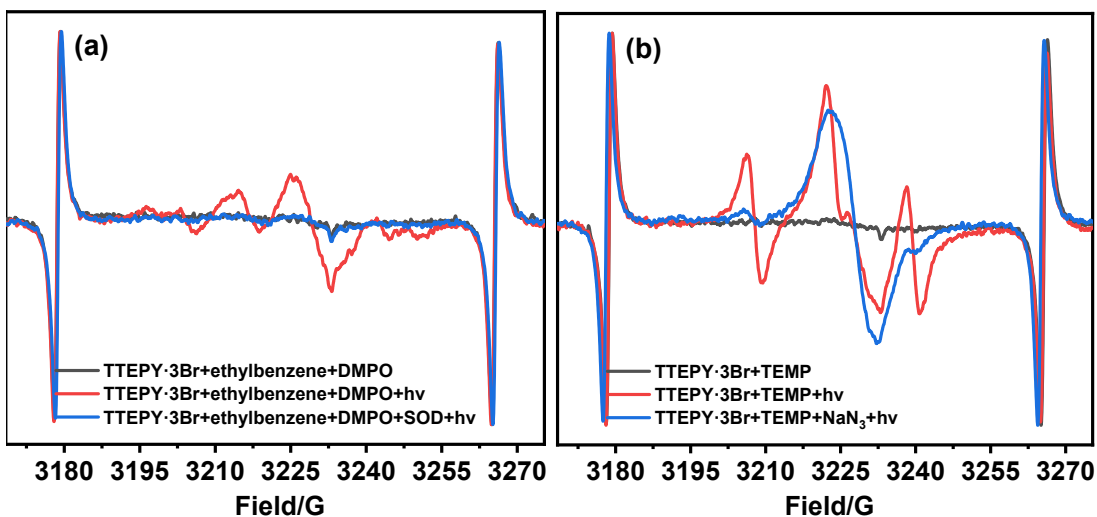


Figure S8. (a) ESR spectra of the samples after mixing DMPO with in the presence of ethylbenzene before and after 365 nm irradiation, as well as photoirradiated sample containing additional SOD. (b) ESR spectra of the samples after mixing TEMP with TTEPY·3Br before and after 365 nm irradiation, as well as photoirradiated sample containing additional NaN₃.

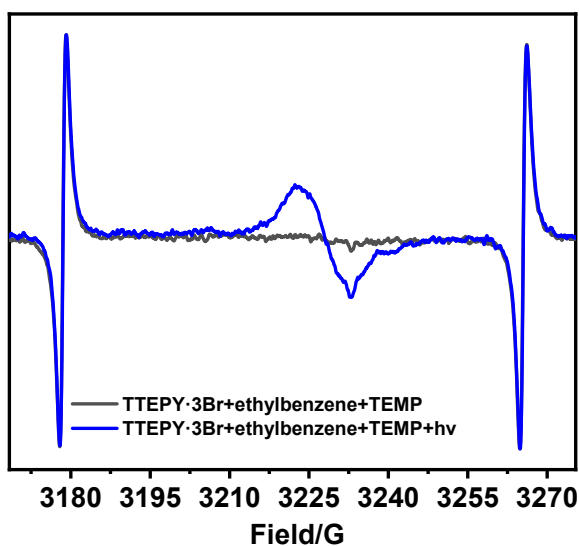


Figure S9. ESR spectra of the mixtures of ethylbenzene and TTEPY·3Br in presence of TEMP before and after 365 nm light irradiation.

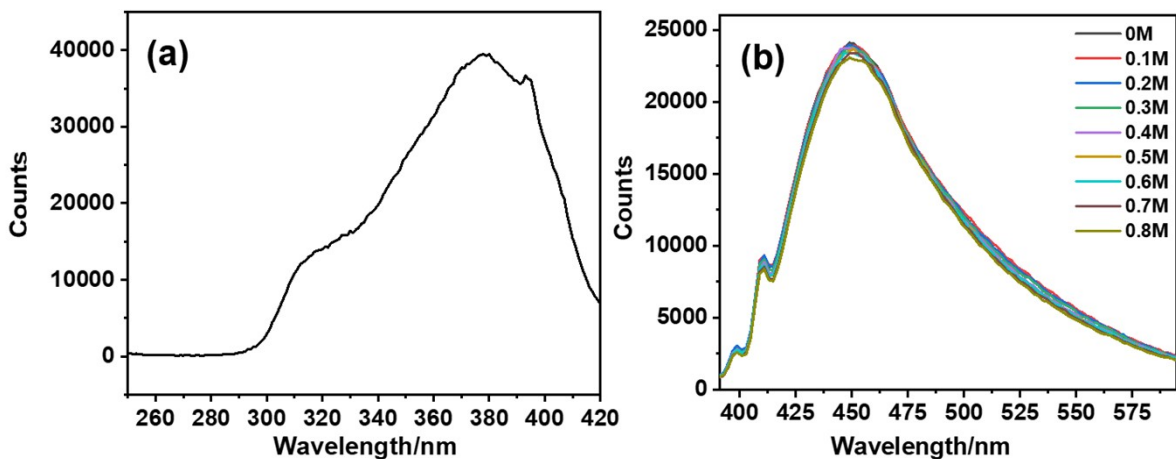


Figure S10. (a) Fluorescence excitation spectrum of TTEPY·3Br; (b) Fluorescence quenching of TTEPY·3Br (5×10^{-4} M) in MeCN in the presence of increasing amounts of ethylbenzene (from 0 to 0.8 M).

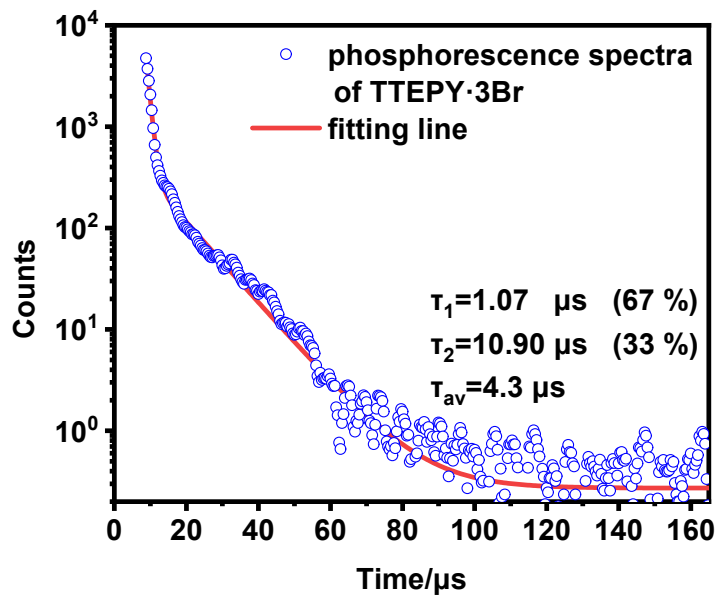


Figure S11. Phosphorescence lifetimes of TTEPY·3Br (5×10^{-4} M) in MeCN. The average lifetime (τ_{av}) was then determined using the equation: $\tau_{av} = \frac{\sum_{i=1}^n a_i \tau_i^2}{\sum_{i=1}^n a_i \tau_i}$

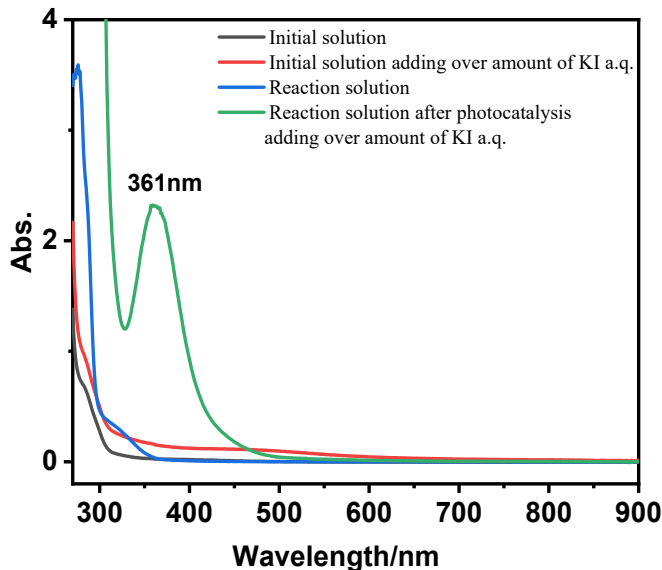


Figure S12. UV-Vis absorption spectra of the tri-iodide formed by H_2O_2 oxidation. The formation of H_2O_2 was confirmed by monitoring tri-iodide (I_3^-) in aqueous solution. When over amount of KI was added to the reaction solution, the characteristic peak of I_3^- ions at ca.361 nm appeared due to the following reactions: [Ref: Huang, W.; Ma, B. C.; Lu, H.; Li, R.; Wang, L.; Landfester, K.; Zhang, K. A. I. *ACS Catal.* **2017**, *7*, 5438-5442]

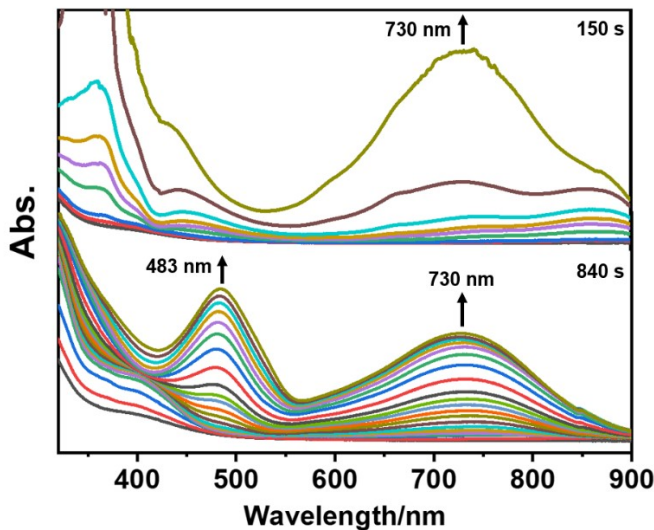
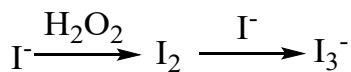


Figure S13. Comparison of the photoinduced absorption spectral changes of TTEPY·3Br (5×10^{-4} M) in MeCN in the presence of 0.5 M 1-phenylethanol (top) or 0.5 M ethylbenzene (bottom) under N_2 atmosphere at room temperature with 365nm light irradiation for different time points.

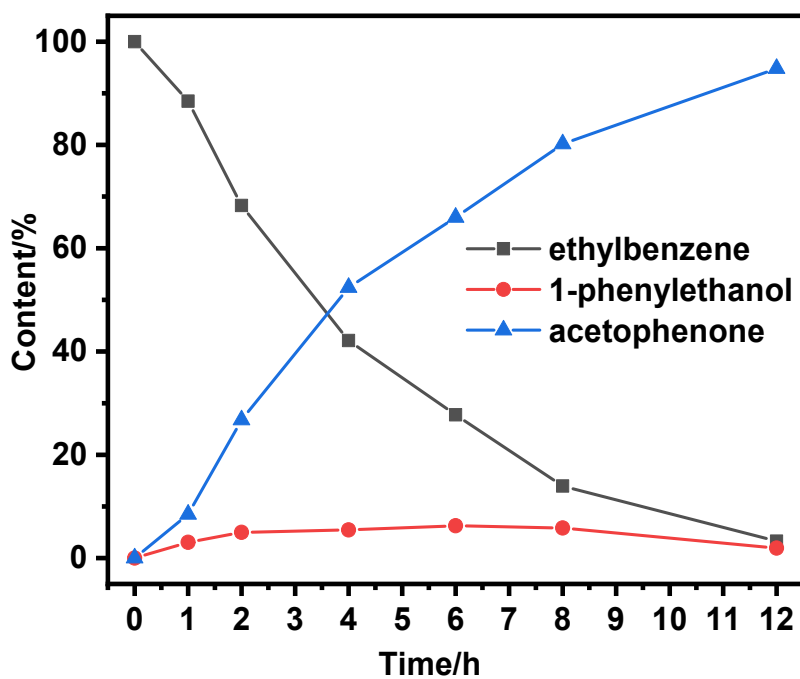


Figure S14. Time courses of the oxidation of ethylbenzene (Reaction conditions: 0.1 mmol ethylbenzene, 2 mol% catalyst, 2 mL acetonitrile, air atmosphere, room temperature, white light irradiation).

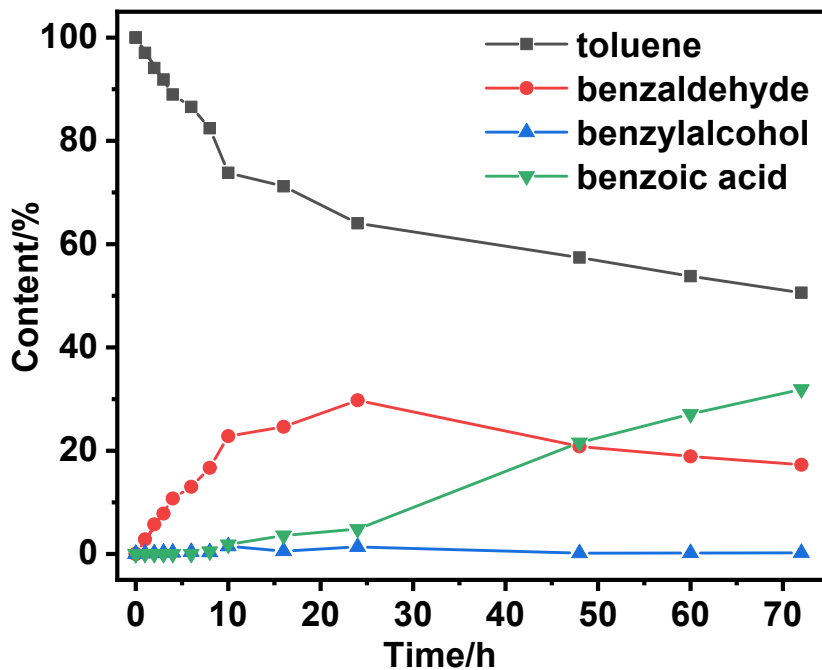
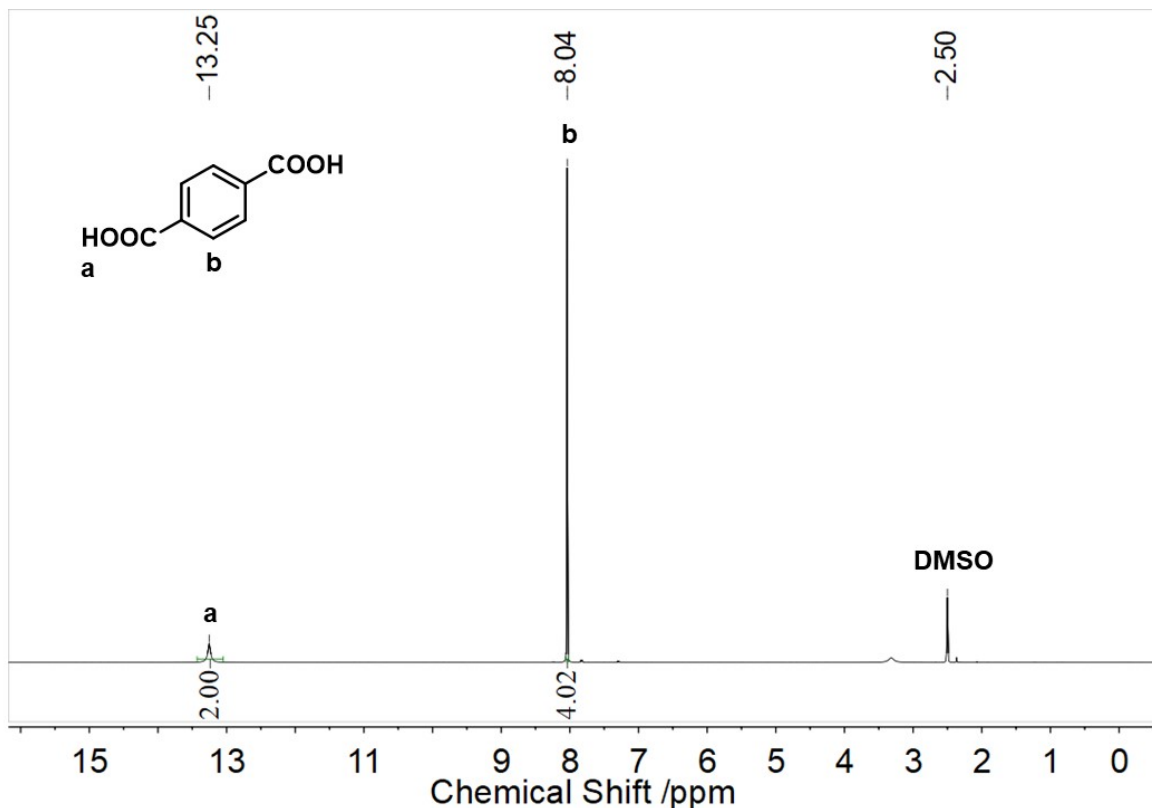


Figure S15. Time courses of the oxidation of toluene (Reaction conditions: 0.1 mmol ethylbenzene, 2 mol% catalyst, 2 mL acetonitrile, air atmosphere, room temperature, white light irradiation).



Before the reaction Photocatalytic reactor After the reaction

Figure S16. The images showing the photocatalytic oxidation of p-xylene into terephthalic acid. The white precipitate can be observed after the reaction.



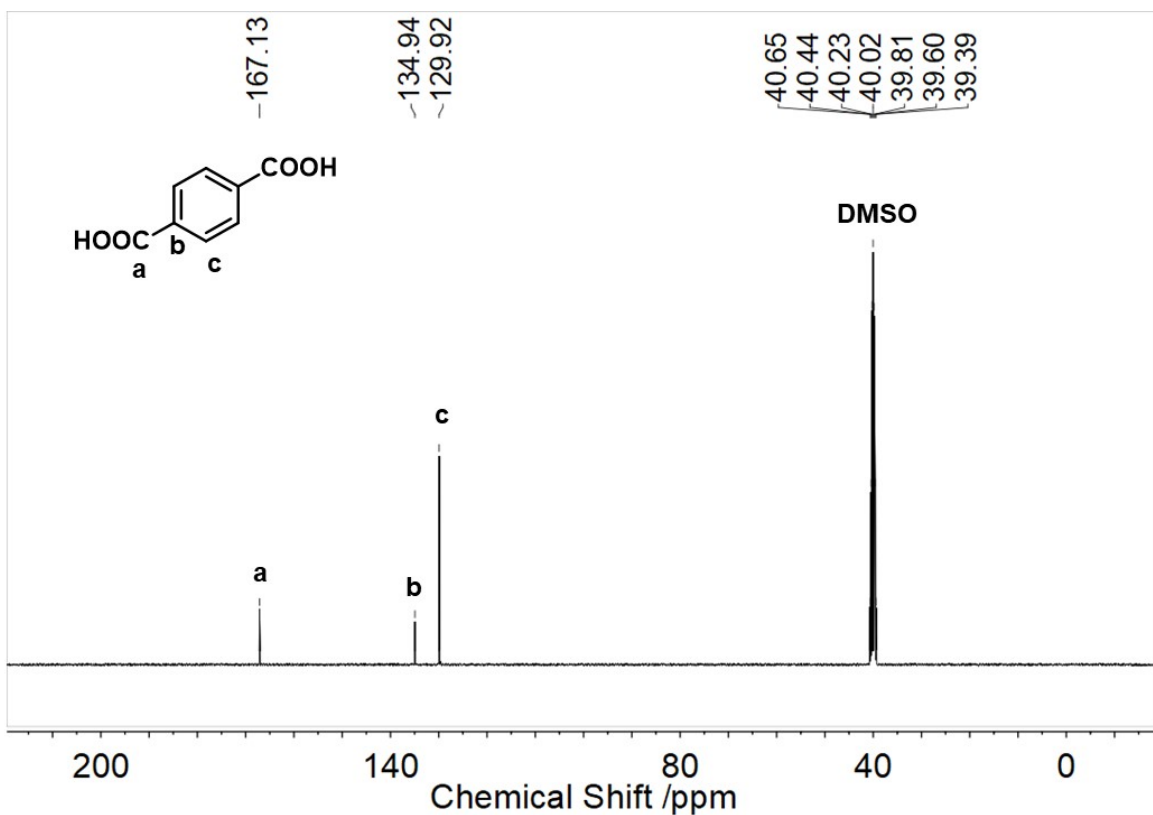


Figure S17. ^1H (top; 400 MHz, DMSO) and ^{13}C (bottom; 100 MHz, DMSO) NMR measurements of the terephthalic acid products (^1H NMR: δ 13.25 (s, 2H), 8.04 (s, 4H); ^{13}C NMR: δ 167.13, 134.94, 129.92)

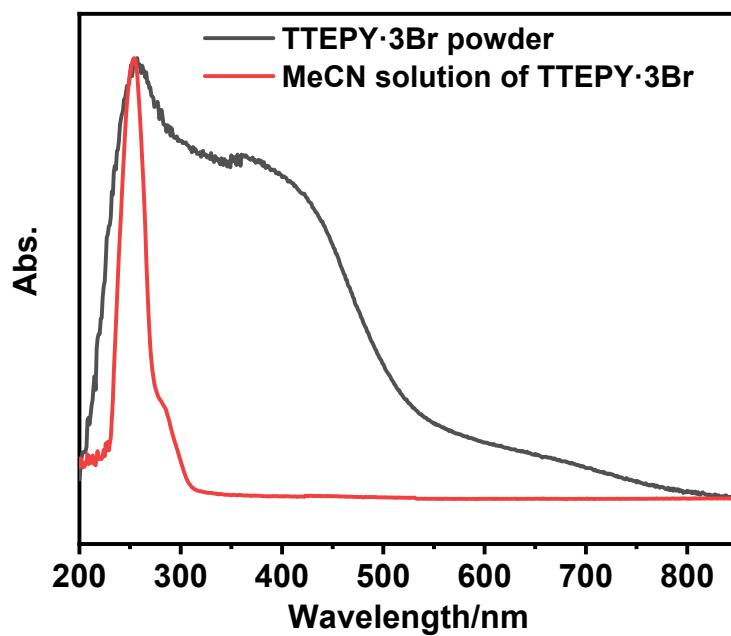


Figure S18. UV-vis absorption spectra of TTEPY·Br in MeCN (3×10^{-5} M) and in the solid state.

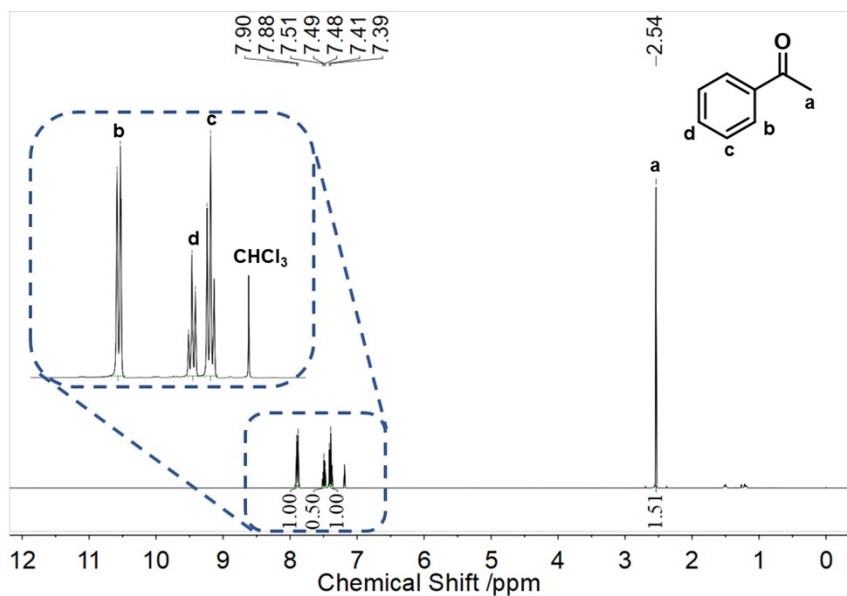
Table S1. General substrate scope for the oxidations under the irritation of white light source.

Entry ^a	Substrate	Product	Time/ h	Yield ^b / %
1			18	96
2			18	92
3			18	94
4			18	95
5			18	>99
6			18	75

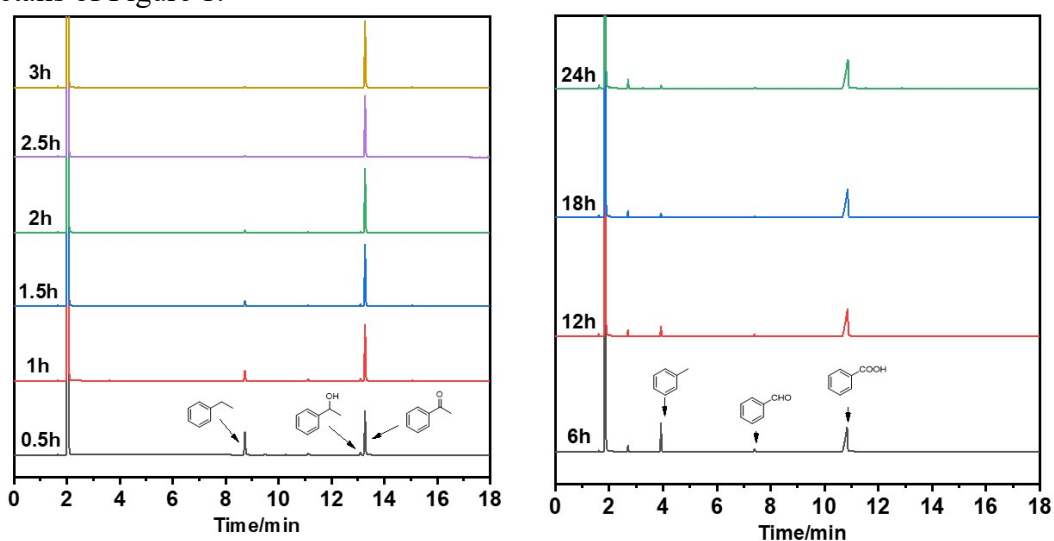
(a) Reaction conditions: substrate: 0.1 mmol; catalyst: 2 mol%, 2 mL acetonitrile; in air condition; room temperature. (b) Determined by GC analysis.

Section 3. NMR, GC, GC-Mass details

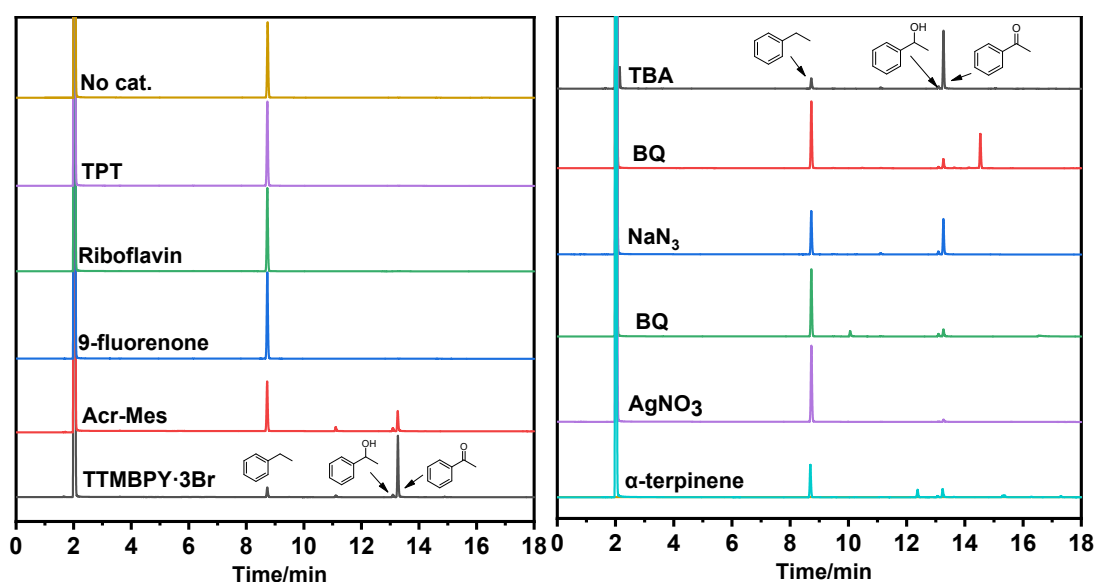
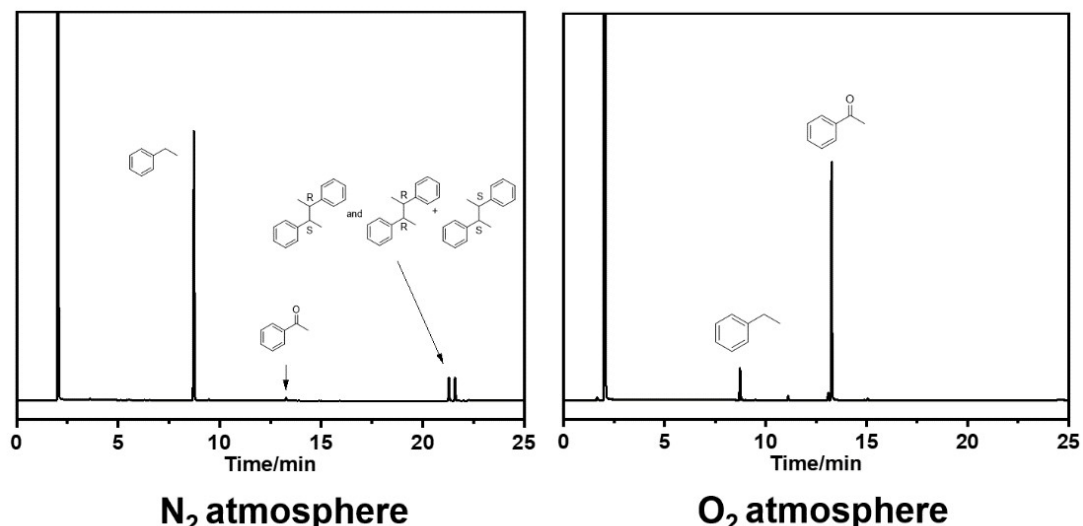
¹H (400 MHz, CDCl₃) NMR measurements of the acetophenone products (¹H NMR: δ 7.89 (d, J = 7.2 Hz, 1H), 7.49 (t, J = 7.4 Hz, 1H), 7.40 (d, J = 7.8 Hz, 1H), 2.54 (s, 2H).



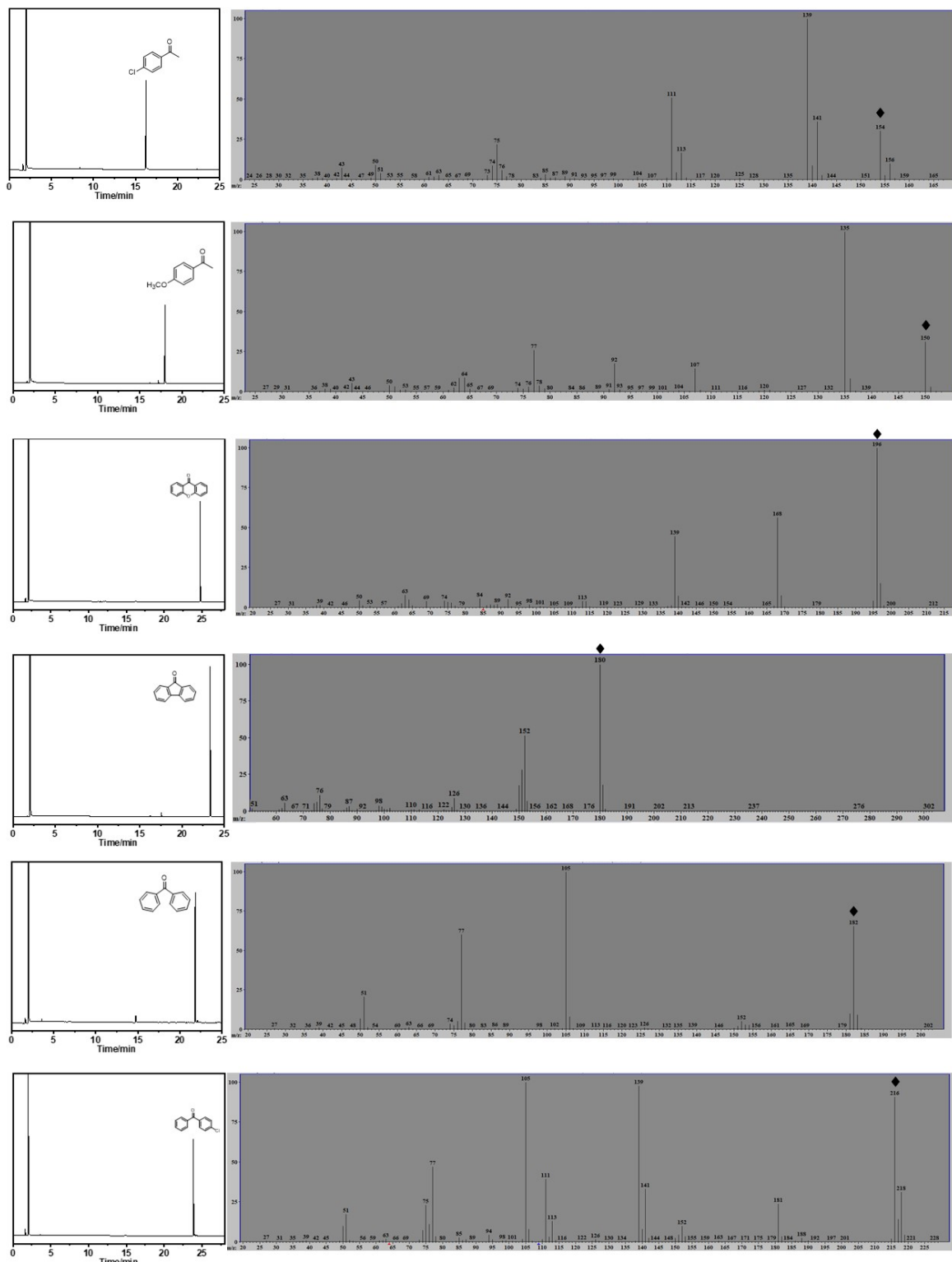
GC details of Figure 1:

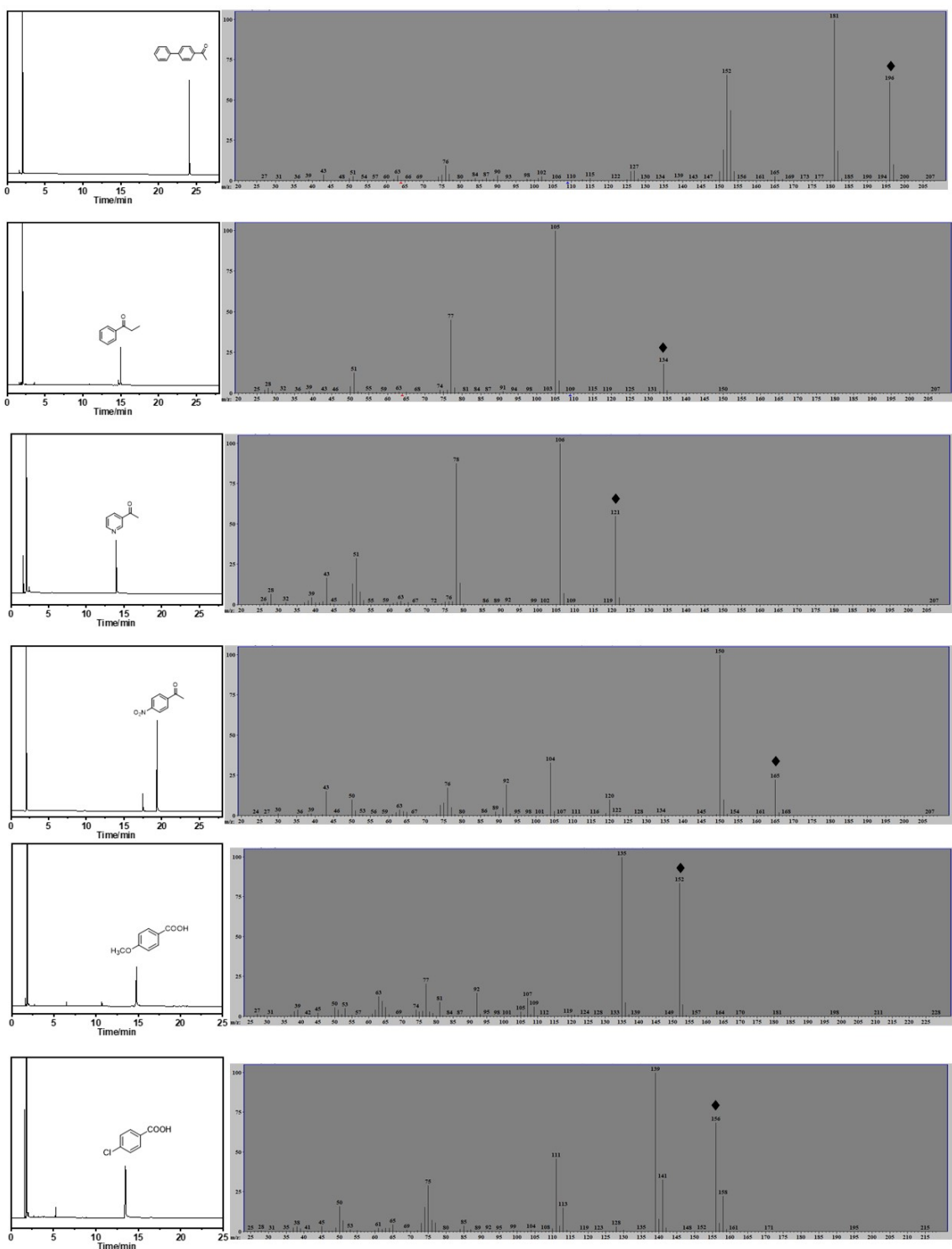


GC details of Table 1 and Figure S8:



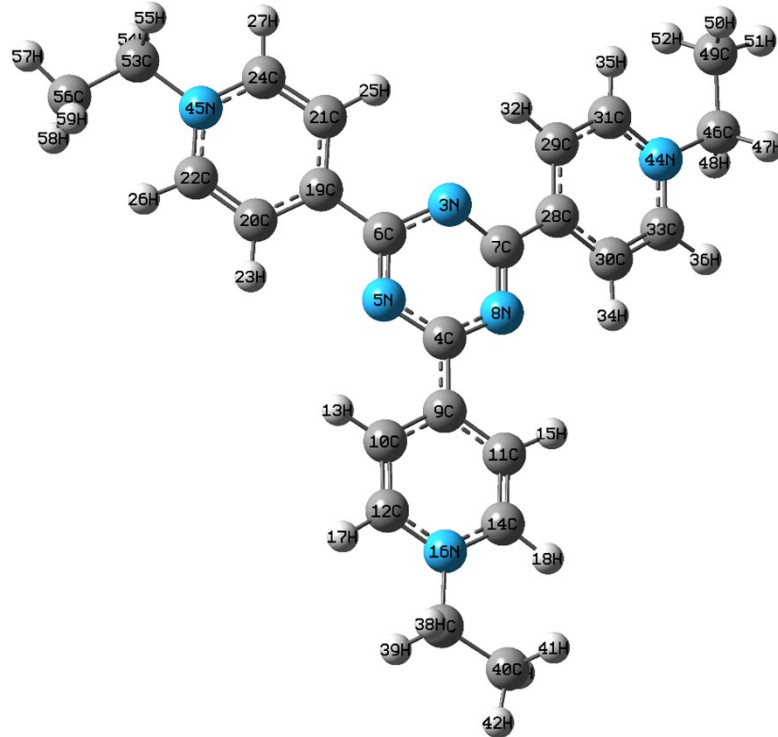
GC, GC-Mass details of Table 2:





Section 4. Spin density details for Cat, Ts-init, Ts and Ts-pro

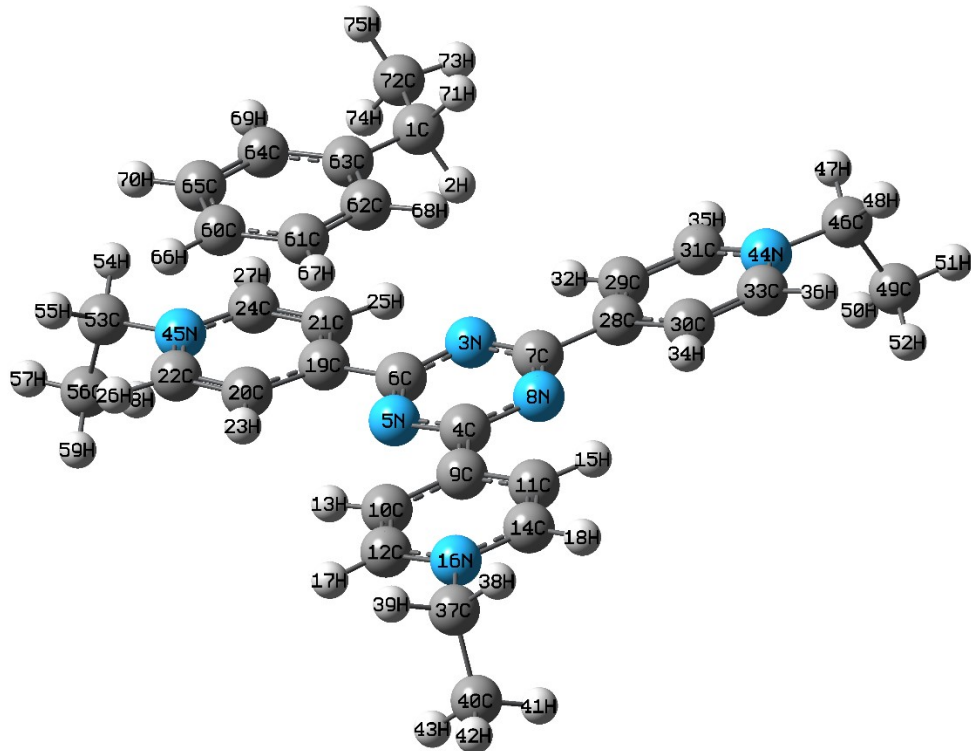
Cat (TTEPY·3Br):



Entry	Element	Spin density
3	N	1.037251
4	C	0.392517
5	N	0.009204
6	C	0.120458
7	C	0.122518
8	N	0.006360
9	C	-0.072386
10	C	0.093616
11	C	0.108419
12	C	-0.027194
13	H	-0.004192
14	C	-0.026835
15	H	-0.004841
16	N	0.102830
17	H	0.000690
18	H	0.000624
19	C	-0.017078
20	C	0.030529

21	C	0.043678
22	C	-0.002775
23	H	-0.001292
24	C	-0.017167
25	H	-0.003573
26	H	-0.000009
27	H	0.000562
28	C	-0.017769
29	C	0.051126
30	C	0.026627
31	C	-0.017537
32	H	-0.004040
33	C	-0.002647
34	H	-0.001150
35	H	0.000531
36	H	-0.000028
37	C	-0.006440
38	H	0.005269
39	H	0.005147
40	C	0.000360
41	H	0.000080
42	H	-0.000163
43	H	0.000074
44	N	0.033499
45	N	0.032293
46	C	-0.002031
47	H	0.001566
48	H	0.001760
49	C	0.000109
50	H	0.000049
51	H	-0.000052
52	H	0.000031
53	C	-0.001942
54	H	0.001772
55	H	0.001457
56	C	0.000145
57	H	-0.000047
58	H	0.000003
59	H	0.000033

Ts-init:

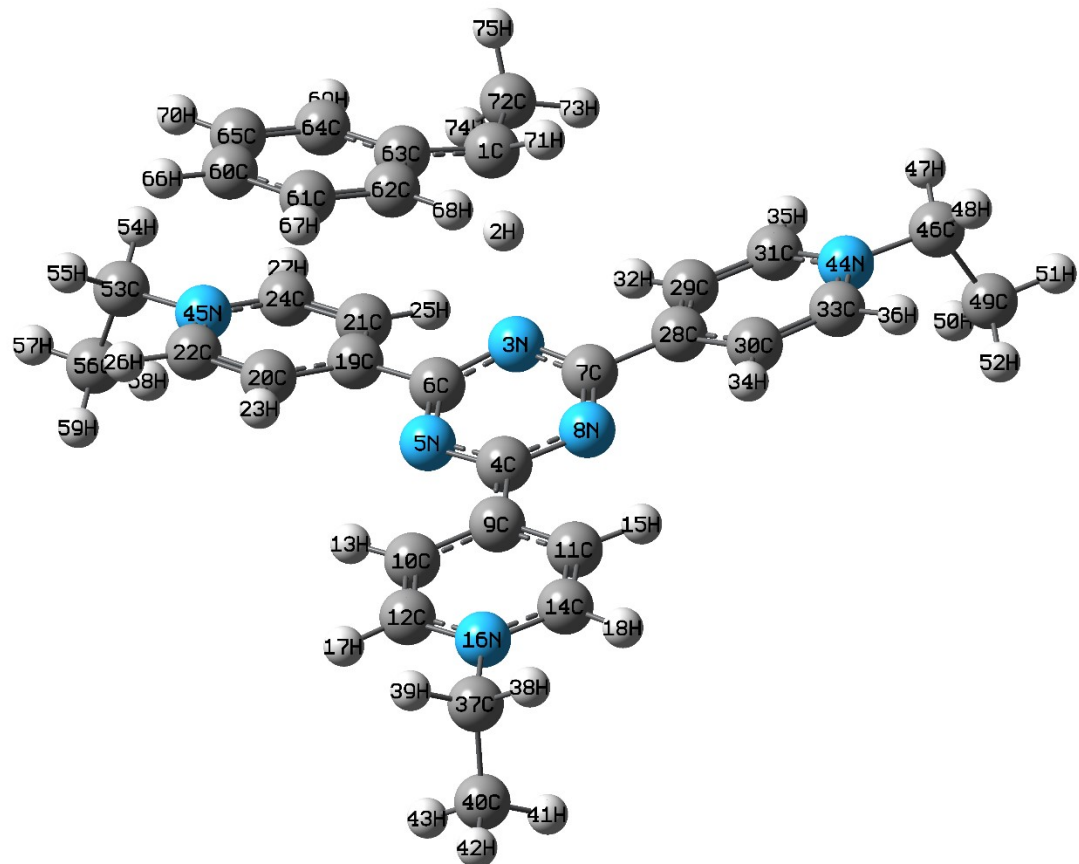


Entry	Element	Spin density
1	C	-0.032248
2	H	0.044647
3	N	0.221576
4	C	0.190857
5	N	0.040547
6	C	0.001901
7	C	-0.005323
8	N	0.054231
9	C	0.103118
10	C	0.067499
11	C	0.065851
12	C	0.025765
13	H	-0.004033
14	C	0.026393
15	H	-0.003991
16	N	0.169389
17	H	-0.001797
18	H	-0.001818
19	C	0.008800

20	C	-0.021673
21	C	0.006045
22	C	0.029104
23	H	0.000810
24	C	0.015495
25	H	-0.000964
26	H	-0.001092
27	H	-0.000698
28	C	0.003902
29	C	0.007307
30	C	-0.002317
31	C	-0.003303
32	H	-0.000979
33	C	0.008300
34	H	-0.000130
35	H	0.000084
36	H	-0.000367
37	C	-0.009758
38	H	0.003396
39	H	0.002470
40	C	0.009762
41	H	-0.000639
42	H	0.001049
43	H	-0.000624
44	N	0.005871
45	N	0.004226
46	C	-0.000308
47	H	0.000081
48	H	0.000104
49	C	0.000331
50	H	-0.000008
51	H	0.000034
52	H	-0.000048
53	C	-0.000262
54	H	0.000062
55	H	0.000102
56	C	0.000452
57	H	0.000035
58	H	-0.000048
59	H	-0.000092

60	C	0.508613
61	C	-0.073213
62	C	0.093634
63	C	0.430179
64	C	0.037442
65	C	-0.021124
66	H	-0.023659
67	H	-0.000322
68	H	-0.006921
69	H	-0.004457
70	H	-0.002141
71	H	0.031093
72	C	0.000224
73	H	-0.000708
74	H	0.002059
75	H	0.002226

Ts:

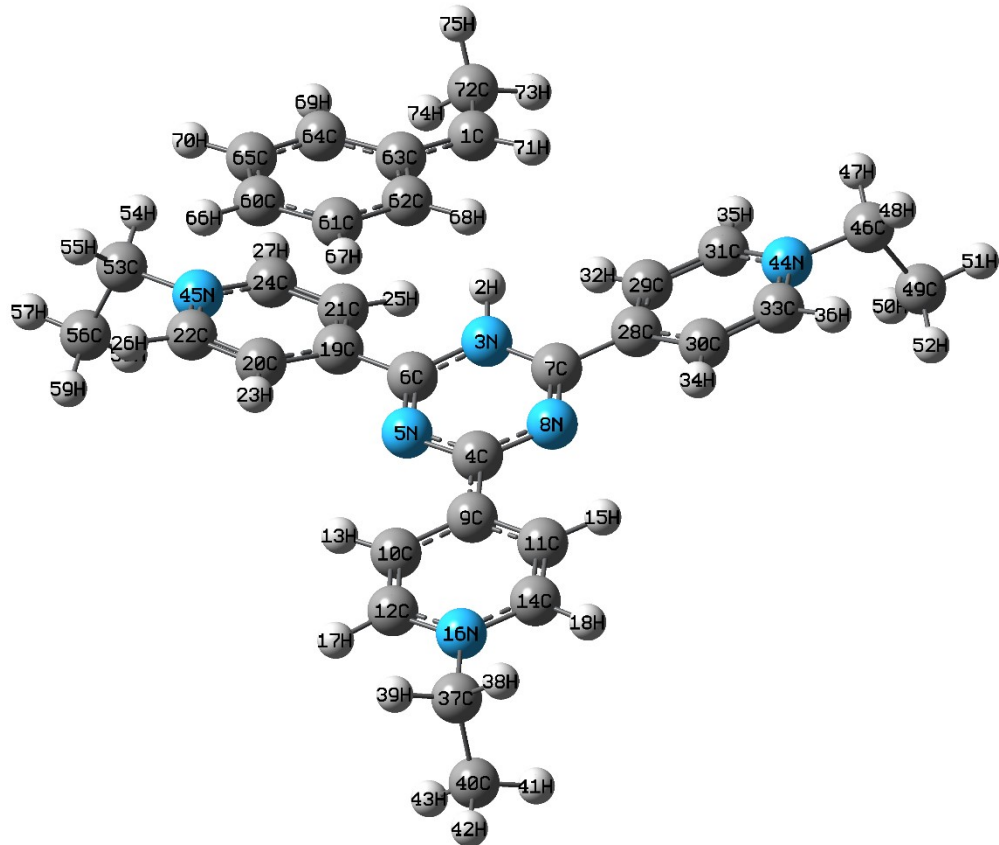


Entry	Element	Spin density
1	C	0.113067
2	H	0.081856
3	N	0.309295
4	C	0.242861
5	N	0.031532
6	C	0.025955
7	C	0.029548
8	N	0.022851
9	C	0.049826
10	C	0.078553
11	C	0.079788
12	C	0.009884
13	H	-0.004256
14	C	0.009958
15	H	-0.004288
16	N	0.152554
17	H	-0.001043
18	H	-0.001051

19	C	-0.008941
20	C	0.003952
21	C	0.023210
22	C	0.005490
23	H	-0.000053
24	C	0.001136
25	H	-0.001367
26	H	-0.000225
27	H	-0.000163
28	C	0.000677
29	C	0.014425
30	C	0.004760
31	C	-0.005954
32	H	-0.000913
33	C	0.006476
34	H	-0.000346
35	H	0.000152
36	H	-0.000321
37	C	-0.008622
38	H	0.002246
39	H	0.002945
40	C	0.008580
41	H	-0.000500
42	H	0.000961
43	H	-0.000517
44	N	0.013980
45	N	0.016771
46	C	-0.000733
47	H	0.000193
48	H	0.000258
49	C	0.000745
50	H	-0.000026
51	H	0.000077
52	H	-0.000065
53	C	-0.000905
54	H	0.000318
55	H	0.000255
56	C	0.000916
57	H	0.000090
58	H	-0.000058

59	H	-0.000059
60	C	0.393147
61	C	-0.102225
62	C	0.166328
63	C	0.171079
64	C	0.140636
65	C	-0.082807
66	H	-0.018293
67	H	0.002044
68	H	-0.008888
69	H	-0.007654
70	H	0.001303
71	H	0.020555
72	C	-0.003250
73	H	-0.000214
74	H	0.005345
75	H	0.017161

Ts-pro:



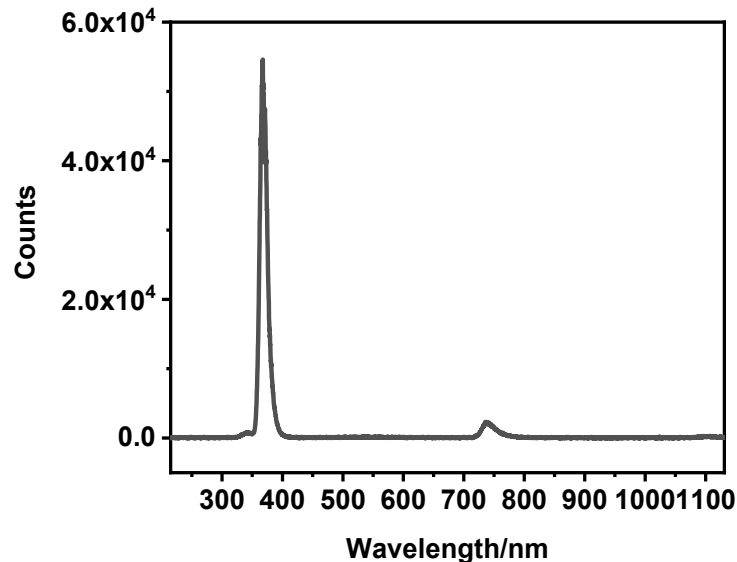
Entry	Element	Spin density
1	C	0.815571
2	H	0.014341
3	N	0.197170
4	C	0.363362
5	N	-0.037304
6	C	0.108265
7	C	0.155903
8	N	-0.076556
9	C	-0.054583
10	C	0.094370
11	C	0.090163
12	C	-0.018625
13	H	-0.004317
14	C	-0.016260
15	H	-0.004115
16	N	0.108127
17	H	0.000321
18	H	0.000244

19	C	-0.014016
20	C	0.013333
21	C	0.029313
22	C	0.002660
23	H	-0.000300
24	C	-0.008954
25	H	-0.002590
26	H	-0.000130
27	H	0.000199
28	C	-0.024668
29	C	0.042202
30	C	0.028410
31	C	-0.014462
32	H	-0.002791
33	C	0.000870
34	H	-0.001303
35	H	0.000391
36	H	-0.000170
37	C	-0.005836
38	H	0.002165
39	H	0.001422
40	C	0.005821
41	H	-0.000272
42	H	0.000712
43	H	-0.000237
44	N	0.036474
45	N	0.021466
46	C	-0.001892
47	H	0.000497
48	H	0.000693
49	C	0.001940
50	H	-0.000066
51	H	0.000225
52	H	-0.000105
53	C	-0.001102
54	H	0.000308
55	H	0.000398
56	C	0.001151
57	H	0.000115
58	H	-0.000044

59	H	-0.000058
60	C	0.227987
61	C	-0.104656
62	C	0.202452
63	C	-0.210477
64	C	0.212131
65	C	-0.106370
66	H	-0.010734
67	H	0.003038
68	H	-0.009976
69	H	-0.010026
70	H	0.003314
71	H	-0.039260
72	C	-0.074954
73	H	0.004212
74	H	0.021632
75	H	0.043841

Section 5. The spectra of the light source used in photocatalytic reaction

The spectra of 365 nm light source:



The spectra of white light source:

